

Received: 30 June 2014 – Accepted: 5 August 2014 – Published: 25 August 2014

Correspondence to: J. Kim (jkim2@yonsei.ac.kr)

Published by Copernicus Publications on behalf of the European Geosciences Union.

ACPD

14, 21709–21748, 2014

**Spatio-temporal
variations in PM₁₀
concentrations over
Seoul**

S. Seo et al.

Title Page

Abstract

Introduction

Conclusions

References

Tables

Figures



Back

Close

Full Screen / Esc

Printer-friendly Version

Interactive Discussion



Abstract

The performance of various empirical linear models to estimate the concentrations of surface-level particulate matter with a diameter less than $10\ \mu\text{m}$ (PM_{10}) was evaluated using Aerosol Robotic Network (AERONET) sunphotometer and Moderate Resolution Imaging Spectroradiometer (MODIS) data collected in Seoul during the Distributed Regional Aerosol Gridded Observation Network (DRAGON)-Asia campaign from March to May 2012. An observed relationship between the PM_{10} concentration and the aerosol optical depth (AOD) was accounted for by several parameters in the empirical models, including boundary layer height (BLH), relative humidity (RH), and effective radius of the aerosol size distribution (R_{eff}), which was used here for the first time in empirical modeling. Results show the strong influence of BLH and R_{eff} on the PM_{10} estimates, while the role of RH was negligible during the campaign period when, in general, RH was lower than in other seasons. A large spatial dependency of the empirical model performance was found by categorizing the locations of the collected data into three different site types, which varied in terms of the distances between instruments and source locations. When both AERONET and MODIS datasets were used in the PM_{10} estimation, the highest correlations between measured and estimated values ($R = 0.76$ and 0.76 using AERONET and MODIS data, respectively) were found for the residential area (RA) site type, while the poorest correlations ($R = 0.61$ and 0.68 using AERONET and MODIS data, respectively) were found for the near source (NS) site type. Significant seasonal variations of empirical model performances for PM_{10} estimation were found using the data collected at Yonsei University (one of the DRAGON campaign sites) over a period of 17 months including the DRAGON campaign period. The best correlation between measured and estimated PM_{10} concentrations ($R = 0.81$) was found in winter, due to the presence of a stagnant air mass and low BLH conditions, which may have resulted in relatively homogeneous aerosol properties within the BLH. On the other hand, the poorest correlation between measured and estimated PM_{10}

Spatio-temporal variations in PM_{10} concentrations over Seoul

S. Seo et al.

Title Page

Abstract

Introduction

Conclusions

References

Tables

Figures



Back

Close

Full Screen / Esc

Printer-friendly Version

Interactive Discussion



**Spatio-temporal
variations in PM₁₀
concentrations over
Seoul**

S. Seo et al.

Title Page

Abstract

Introduction

Conclusions

References

Tables

Figures



Back

Close

Full Screen / Esc

Printer-friendly Version

Interactive Discussion



2010; Wang et al., 2010), correlations between measured and predicted PM_{2.5} were further improved when compared with correlations obtained from linear models using only AOD. A multiple linear regression model between measured and predicted PM_{2.5} concentrations in urban areas yielded a correlation of 0.71 (Liu et al., 2007). Spatial distributions of PM_{2.5} can also be estimated by applying the ratio of AOD to PM_{2.5}, as calculated from chemical transport models (CTM), such as the Goddard Earth Observing System-Chemistry (GEOS-CHEM) transport model and the Community Multiscale Air Quality (CMAQ) model (Liu et al., 2004; van Donkelaar et al., 2010). These previous studies have demonstrated the strong possibility of deriving surface PM concentrations from AOD data.

However, if we are to further improve and validate PM estimates, additional physical parameters should be considered as inputs into the empirical models, so as to obtain accurate estimates of PM concentrations from AOD data. Additionally, the effects of various environmental characteristics on the relationship between PM and AOD, as well as spatial and temporal variations in this relationship, need to be investigated, especially in complex urban regions which include aerosol particles generated from various industrial and residential sources. Despite the need to monitor the rapidly changing PM concentrations in megacities with large populations and many sources of pollution, only a small number of studies have been conducted, especially in Asia, and the numbers of ground-based PM monitoring stations in these studies has been limited (Kumar et al., 2007; Guo et al., 2009). In addition to limitations based on sample size, obtaining accurate estimates of PM from AOD data has proved difficult in Asia on account of the complexity of the aerosol compositions derived from both natural and anthropogenic sources, particularly during the spring (Kim et al., 2007; Lee et al., 2010a).

In an effort to address these problems, the present study uses aerosol measurements collected during the Distributed Regional Aerosol Gridded Observation Network (DRAGON)-Asia 2012 campaign, which is just one of the DRAGON campaigns that has been conducted globally (http://aeronet.gsfc.nasa.gov/new_web/DRAGON-Asia_2012_Japan_South_Korea.html). The intensive DRAGON campaigns have provided

Spatio-temporal variations in PM₁₀ concentrations over Seoul

S. Seo et al.

Title Page

Abstract

Introduction

Conclusions

References

Tables

Figures



Back

Close

Full Screen / Esc

Printer-friendly Version

Interactive Discussion



valuable datasets, with well-coordinated measurements made in areas where aerosol concentrations are highly variable in space and time, and dependent on sources and other factors. The DRAGON campaigns have been conducted in urban and industrial areas, including Washington D.C., San Joaquin Valley of California, and Houston metropolitan region of Texas. By using the campaign datasets obtained from the dense coverage of both column and surface-level aerosol measurements, assessments of surface-level PM concentrations based on remote sensing observations can be substantially improved, especially in spring.

The purpose of this study is to investigate the relationship between AOD and PM concentrations in Seoul, one of the largest megacities in northeast Asia, using the DRAGON-Asia campaign dataset. The detailed objectives of this study are: (1) to estimate PM₁₀ concentrations using AOD data from both ground- and satellite-based measurements in a megacity, with additional consideration of the various parameters within the empirical models, and to thereby evaluate derived PM concentrations; (2) to identify the spatial variability of the empirical model performance at different types of measurement site; and (3) to investigate the seasonal variability of the performance of each model. Based on this study, it is expected that PM₁₀ estimations using ground-based and satellite-derived AOD data will become an effective approach to monitoring air quality over large spatial domains, especially in complex urban areas.

2 Measurements during the DRAGON-Asia campaign

The study area, Seoul, is a megacity located in a downwind region of northeast Asia, in which air quality is often affected by both pollutants transported over long distances from continental interior and locally generated aerosol. The present study used the column aerosol optical properties measured at 10 Aerosol Robotic Network (AERONET) sites in Seoul, as well as those obtained by a dense mesoscale network of ground-based instruments during the DRAGON-Asia 2012 campaign, which was conducted over the three-month period March–May 2012 (Fig. 1). The hourly-averaged PM₁₀ con-

centrations were also measured at 10 sites operated by a national air quality monitoring network during the campaign (<http://www.airkorea.or.kr>).

2.1 Column AOD and surface PM measurements

The AERONET sunphotometers (<http://aeronet.gsfc.nasa.gov/index.html>), which provide aerosol optical and microphysical properties based on direct sun and diffuse sky measurements (Holben et al., 1998), have been widely used as references for measurements from different satellite platforms. The AOD and the Angstrom exponent (AE) can be retrieved from direct sun measurements in several spectral bands, usually between 340 and 1020 nm (Holben et al., 1998). Diffuse sky measurements, which are performed at a minimum of four wavelengths (440, 670, 870, and 1020 nm), use an inversion method to provide detailed aerosol properties, such as the size distribution, phase function, single scattering albedo, refractive index, etc. (Holben et al., 1998; Dubovik and King, 2000). The AOD at 550 nm was obtained from AERONET level 2.0 direct sun measurements (cloud-screened and quality assured) at seven sites, and level 1.5 products (cloud-screened) at three sites. In addition to the AERONET AOD, the effective radius for the total (fine and coarse modes) size distribution obtained from the inversion product was also used to represent the aerosol size information in the empirical regression models (Dubovik and King, 2000). Although cloud-screened AERONET data were used, additional cloud screening was performed for further quality control using the cloud amount data provided by the Korea Meteorological Administration (KMA; <http://www.kma.go.kr>) and the attenuated backscattering signal measured from the two-wavelength Mie lidar located at Seoul National University (SNU). A cloud-free sky condition was defined as a cloud amount of less than 20 % (cf. Ogunjobi et al., 2004) and no detections of strong scattering peaks of lidar measurements due to clouds. AOD measurements from the Moderate Resolution Imaging Spectroradiometer (MODIS) on board the Terra and Aqua satellites were also used to formulate the empirical regression models (Remer et al., 2005; Levy et al., 2007). To identify the optimal grid size for the MODIS AOD in this mesoscale spatial domain, the collocation

Spatio-temporal variations in PM₁₀ concentrations over Seoul

S. Seo et al.

Title Page

Abstract

Introduction

Conclusions

References

Tables

Figures



Back

Close

Full Screen / Esc

Printer-friendly Version

Interactive Discussion



tance of approximately 4.5 km) were used. On the other hand, the MODIS AOD data, which were measured at different spatial grid resolutions, were extracted within a maximum distance of 0.2° of the PM_{10} measurement sites. The AERONET and MODIS AOD were both temporally collocated within ± 30 min of the hourly PM_{10} measurement time.

2.2 Meteorological measurements

Meteorological data were used to investigate the relationship between AOD and PM_{10} concentrations. The attenuated backscatter coefficient at 532 nm, measured by the two-wavelength Mie lidar located at Seoul National University (<http://www-lidar.nies.go.jp/Seoul/>), was used to calculate the hourly BLH using the automated wavelet covariance transform (WCT) method (Brooks, 2003). The WCT method was applied to backscattered lidar signals at heights above 300 m from the surface to avoid the problem of uncertainty in lidar overlap (Campbell et al., 2002). Figure 3 shows an example of temporal variation in the BLH obtained by application of the WCT method.

In addition to the BLH, other meteorological data such as temperature, relative humidity, cloud amount, and wind speed and direction were obtained from hourly measurements at a KMA weather observation station in Seoul (37.57° N, 126.97° E). All meteorological data within ± 30 min of the PM_{10} observation time were used for this investigation.

3 Methodology

3.1 Relationship between column AOD and surface PM concentration

The AOD is the integration of the radiative extinction due to aerosols from the surface up to the top of the atmosphere (TOA) at a given wavelength. The AOD can be defined

Spatio-temporal variations in PM_{10} concentrations over Seoul

S. Seo et al.

Title Page

Abstract

Introduction

Conclusions

References

Tables

Figures



Back

Close

Full Screen / Esc

Printer-friendly Version

Interactive Discussion



Spatio-temporal variations in PM₁₀ concentrations over Seoul

S. Seo et al.

Title Page

Abstract

Introduction

Conclusions

References

Tables

Figures



Back

Close

Full Screen / Esc

Printer-friendly Version

Interactive Discussion



In Eq. (3), various physical parameters are involved in the relationship between AOD and PM₁₀. The PM₁₀ concentration is proportional to AOD, R_{eff} , and particle mass density ρ ; on the other hand, PM₁₀ is inversely proportional to BLH, $f(\text{RH})$, and (Q_{ext}) . Among these parameters, BLH and $f(\text{RH})$ have been used as parameters in empirical models to estimate PM concentrations using AOD data, as described in Table 1. On the other hand, parameters such as ρ , R_{eff} , and (Q_{ext}) have been rarely included in empirical models. In the present study, the effective radius of the aerosol size distribution was included for the first time as an additional parameter in the empirical models. The empirical models, and the parameters considered in those models, are described in detail in Sect. 3.2.

3.2 Description of empirical linear models for PM₁₀ estimation

Table 3 presents a summary of the various models used in this study. Models M1 to M5 are empirical models based on the relationship between AOD and PM concentration, as described in Sect. 3.1, whereas M6 represents a multiple linear regression model. Among the empirical models, M1, M2, and M4 have been used in previous studies (e.g., Chu et al., 2003; Wang and Christopher, 2003; Engel-Cox et al., 2004, 2006; Koelemeijer et al., 2006; Gupta and Christopher, 2008; Schaap et al., 2009; Emili et al., 2010; Wang et al., 2010). Model M1 includes only AOD as a predictor of the PM₁₀ concentration, while M2 additionally includes BLH to consider the aerosol vertical extension. The vertical correction on AOD is represented in M2 by dividing AOD by BLH, with the assumption that aerosols within the boundary layer are homogeneously mixed. Model M4 corrects for RH by using an aerosol hygroscopic growth factor term $f(\text{RH})$ which represents the effects of aerosol hygroscopic growth caused by variations in relative humidity, in addition to the parameters in M2. In this study, $f(\text{RH})$ values were based on experimental data obtained near the Beijing mega-city during the spring (Pan et al., 2009). Models M3 and M5, which also included the parameters used in M1, M2, and M4, were the first empirical models to include the effective radius of the aerosol size distribution as a size correction factor. Model M3 includes the aerosol effective radius in

addition to the parameters in M2 to account for the size of aerosol particles. Model M5 reflects all parameters, including AOD, $f(\text{RH})$, BLH, and the effective radius, as shown in Table 3. The effective radius of the aerosol size distribution for the total mode, which was used in M3 and M5, was obtained from AERONET inversion products (Dubovik and King, 2000; Dubovik et al., 2000).

In addition to the simple empirical models (M1–M5), a multiple linear regression (MLR) model was used to determine PM_{10} concentrations as a function of eight different parameters associated with PM estimation:

$$[\text{PM}_{10}] = \exp(\beta_0) \times (\text{AOD})^{\beta_{\text{AOD}}} (\text{BLH})^{\beta_{\text{BLH}}} (\text{AE})^{\beta_{\text{AE}}} \times \exp[\beta_{\text{loc}}(\text{Location}) + \beta_{\text{WS}}(\text{WS}) + \beta_{\text{WD}}(\text{WD}) + \beta_{\text{RH}}(\text{RH}) + \beta_{\text{Temp}}(\text{Temp})] \quad (4)$$

This MLR model of Eq. (4) can be log-transformed into a simpler form of linear regression as shown in Eq. (5).

$$\ln[\text{PM}_{10}] = \beta_0 + \beta_{\text{AOD}} \ln(\text{AOD}) + \beta_{\text{BLH}} \ln(\text{BLH}) + \beta_{\text{AE}} \ln(\text{AE}) + \beta_{\text{loc}}(\text{Location}) + \beta_{\text{WS}}(\text{WS}) + \beta_{\text{WD}}(\text{WD}) + \beta_{\text{RH}}(\text{RH}) + \beta_{\text{Temp}}(\text{Temp}) \quad (5)$$

The dependent variable in Eq. (5) is the logarithm of the hourly PM_{10} concentration measured at the PM monitoring sites. The independent variables include aerosol optical properties such as AOD and AE, various meteorological measurements such as BLH, temperature (Temp), and wind speed (WS), and two categorical variables: type of measurement site (Location) and wind direction (WD). To represent the effect of aerosol size on PM_{10} concentration, AE was used as a variable in the MLR model instead of R_{eff} , because the size of the R_{eff} dataset ($N = 713$) was considered inadequate as compared with that available for AE ($N = 2112$); thus, the use of AE improves the performance of the MLR model and increases the credibility of the model results. Measurement sites were categorized into three types: near source (NS), typical urban (TU), and residential area (RA), as shown in Fig. 1. The NS sites were those located within 500 m of sources; sources in this case included traffic-congested roads and industrial

Spatio-temporal variations in PM_{10} concentrations over Seoul

S. Seo et al.

Title Page

Abstract

Introduction

Conclusions

References

Tables

Figures

◀

▶

◀

▶

Back

Close

Full Screen / Esc

Printer-friendly Version

Interactive Discussion



complexes. The TU sites were located more than 500 m from sources, in either commercial or residential areas. The RA sites were located more than 500 m from sources and in residential areas only. Wind directions were classified as east, south, west, or north. Regression coefficients (β) were determined for each of the independent variables. This MLR analysis was conducted using AERONET dataset only, because this was sufficient to yield credible results.

For an unbiased assessment of model performance, the entire AERONET dataset was randomly divided into two groups, a modeling group ($N = 1058$ for M1, M2, M4, and M6, and $N = 369$ for M3 and M5) that was used to develop the empirical models, and a validation group ($N = 1054$ for M1, M2, M4, and M6, and $N = 373$ for M3 and M5) that was used to validate these models. To minimize the effects of temporal autocorrelation, data were selected such that the time interval between validation and modeling data was at least 24 h. Summary statistics for the variables involved in the modeling and validation datasets are shown in Fig. 4. All empirical models for hourly PM_{10} estimates based on the AERONET datasets were fitted using the modeling dataset to estimate the model coefficients. Estimated regression coefficients (β), standard errors, and p -values of parameters used in M6 (Eq. 5) are summarized in Table 4. As shown in Table 4, most parameters used in M6 were found to be highly significant ($p < 0.0001$) predictors of the PM_{10} concentration. The positive sign of the coefficient for AOD (0.527 ± 0.022) shows a direct correspondence between AOD and surface PM_{10} , given that other conditions remained constant. On the other hand, the estimated power of the BLH relationship was negative (-0.280 ± 0.028), which indicates an inverse relationship between BLH and the PM_{10} concentration. The reason for this inverse relationship is that a lower BLH confines aerosols to a thinner atmospheric layer, resulting in higher surface PM_{10} concentrations. A negative coefficient was also obtained for RH (-0.610 ± 0.116), showing that higher RH conditions result in lower PM_{10} concentrations (given constant AOD values); i.e., the effect of aerosol hygroscopic growth is reflected in the MLR model (M6).

Spatio-temporal variations in PM_{10} concentrations over Seoul

S. Seo et al.

Title Page

Abstract

Introduction

Conclusions

References

Tables

Figures

◀

▶

◀

▶

Back

Close

Full Screen / Esc

Printer-friendly Version

Interactive Discussion



Spatio-temporal variations in PM₁₀ concentrations over Seoul

S. Seo et al.

Title Page

Abstract

Introduction

Conclusions

References

Tables

Figures

◀

▶

◀

▶

Back

Close

Full Screen / Esc

Printer-friendly Version

Interactive Discussion



that a vertical correction on AOD using the BLH value improves PM₁₀ estimates. The correlations between measured and estimated PM₁₀ using M2 with MODIS data are slightly higher than those obtained in the previous work of Emili et al. (2010), which was based on a combination of Spinning Enhanced Visible and Infrared Imager (SE-VIRI) and MODIS AOD data to estimate hourly PM₁₀ concentrations over the European Alpine regions. The differences between the results of Emili et al. (2010) and those obtained here could be associated with uncertainties in surface reflectance in alpine regions that resulted in relatively larger errors in the alpine AOD data as compared with those obtained in Seoul.

Aerosol effective radius data obtained from AERONET measurements was used as a parameter in model M3 to estimate PM₁₀. The effective radius of aerosol, as derived from sky radiances obtained from solar almucantar measurements, is available only when the solar zenith angle (SZA) is larger than 50° (except for near local noon), which avoids polarization effects (Holben et al., 1998; Dubovik and King, 2000). Consequently, in contrast to the AOD data, the effective radius data is available only in a limited time window. The limited number of effective radius measurements was used as an input to M3 to estimate PM₁₀; we used 35.4% ($N = 373$) of the total number of AERONET validation datasets ($N = 1054$) in which data were simultaneously available for both AOD and the effective radius. Model M3 was not implemented using MODIS AOD due to a lack of effective radius information in the MODIS datasets over land areas. As shown in Table 5, the correlation between measured PM₁₀ and those estimated from M3 is higher than that obtained using M2 with the same number of datasets ($N = 373$; $R_{M3,AERO} = 0.55$, $R_{M2,AERO} = 0.46$). Although the results are subject to further validation, aerosol size corrections using the effective radius (M3), in general, lead to better estimates of PM₁₀ concentrations than do those without (M2), at least during the time frame of the intensive campaign period.

Model M4, which incorporates the aerosol hygroscopic growth factor ($f(RH)$) in PM₁₀ estimation, yields a correlation coefficient of 0.63 (0.71) for the AERONET (MODIS) dataset (Table 5). These correlations are similar to those obtained using M2, in which

Spatio-temporal variations in PM₁₀ concentrations over Seoul

S. Seo et al.

[Title Page](#)[Abstract](#)[Introduction](#)[Conclusions](#)[References](#)[Tables](#)[Figures](#)[◀](#)[▶](#)[◀](#)[▶](#)[Back](#)[Close](#)[Full Screen / Esc](#)[Printer-friendly Version](#)[Interactive Discussion](#)

among those calculated with the empirical models (Table 5). The RMSE values between measured PM₁₀ concentrations and those estimated using M1_{cl} ($N = 1054$), M2 ($N = 1054$), and M4 ($N = 1054$), based on the same number of AERONET datasets as inputs, are 23.79, 22.11, and 22.11 $\mu\text{g m}^{-3}$, respectively, showing that the models tend to improve (i.e., the errors tend to decrease) when using the BLH as a predictor in the empirical models. This improvement in the models was also found when a vertical correction is applied to the MODIS data. The RMSE values of PM₁₀ estimated using M1_{cl} ($N = 252$), M2 ($N = 252$), and M4 ($N = 252$), and based on inputs of MODIS data, were 28.55, 23.02, and 23.19 $\mu\text{g m}^{-3}$, respectively. The RMSE values of PM₁₀ estimated using M2 ($N = 373$), M3 ($N = 373$), and M5 ($N = 373$), and based on the same number of AERONET datasets, were 23.27, 22.01, and 21.32 $\mu\text{g m}^{-3}$, respectively, when a size correction using the aerosol effective radius and an RH correction using the particle hygroscopic growth factor were incorporated into the models. To evaluate the empirical model performance for PM₁₀ estimation, the mean normalized bias (MNB) and the mean fractionalized bias (MFB) were also calculated (these statistical parameters are described in the footnote of Table 5). The tendencies of both the MNB and MFB are similar to those of the RMSE, except for M6. All MFB values (except for M6) are positive, which indicates that the PM₁₀ concentrations derived from the models are generally overestimated when compared with measured PM₁₀ values. The MFB of M6 was -0.83% , which shows that M6 tends to underestimate the PM₁₀ concentration, especially at high concentrations on account of the log transformation of the data.

4.2 Spatial characteristics of correlations between measured and estimated PM₁₀

Large variations in the mean and standard deviation of the measured PM₁₀ concentrations were observed, with the size of the deviations dependent on the measurement site type. As described in Sect. 3.2, the site types include near source (NS), typical urban (TU), and residential area (RA) site types in Seoul, as identified during the DRAGON-Asia campaign. The means (standard deviations) of the hourly measured

Spatio-temporal variations in PM₁₀ concentrations over Seoul

S. Seo et al.

Title Page

Abstract

Introduction

Conclusions

References

Tables

Figures

◀

▶

◀

▶

Back

Close

Full Screen / Esc

Printer-friendly Version

Interactive Discussion



highest correlations for the RA site type, while the lowest are for the NS sites. The correlation coefficients for the RA sites were between 0.50 and 0.76 for models M1_{cl}, M2, and M4, whereas those for the TU and NS sites were 0.42–0.72 and 0.37–0.68, respectively. The highest correlation between measured and estimated PM₁₀, obtained using M2 with MODIS data, was comparable with those obtained using M5 and M6 with AERONET data. This high performance of the empirical models using the MODIS data can be explained by the overpass time of the MODIS data, which was around midday when aerosols are generally well-mixed within the boundary layer compared with other times of the day (Schaap et al., 2009).

The inverse distance weighting (IDW) interpolation method was applied to estimate the PM₁₀ concentrations using M2 with MODIS AOD data over various campaign sites, at a spatial resolution that was finer than that established for the original MODIS data (10 km). The IDW method was used to estimate PM₁₀ concentrations in alpine regions with simple PM source distributions (Emili et al., 2010). In this study, model M2 with MODIS AOD and lidar BLH data was used to estimate PM₁₀ concentrations at a resolution of 0.02° (ca. 2 km) over the Seoul area. Slopes and intercepts of M2 were spatially interpolated to a resolution of 0.02° using the IDW method, as calculated from values at the four closest pixels. Figure 5 shows PM₁₀ estimates at the 2 km resolution based on the IDW method, where the colored circles represent PM₁₀ concentrations measured at PM monitoring sites. The spatial distribution of the estimated and measured PM₁₀ concentrations is generally in good agreement. However, a discontinuity is observed in Fig. 5, which could be due to a problem associated with AOD input at a low resolution and its interpolation based on inhomogeneous sampling of a small number of data points.

4.3 Seasonal characteristics of correlations between measured and estimated PM₁₀

The empirical models proposed in Sect. 3.2 were applied to data collected for an extended time period (beyond that of the DRAGON-Asia campaign) at a Yonsei University

Spatio-temporal variations in PM₁₀ concentrations over Seoul

S. Seo et al.

Title Page

Abstract

Introduction

Conclusions

References

Tables

Figures



Back

Close

Full Screen / Esc

Printer-friendly Version

Interactive Discussion



AERONET and MODIS data occurred for the RA sites, while the lowest was for the NS sites, where the spatio-temporal variability of aerosols is high. The selection of site types either dominates, or is comparable with, the specific empirical model selected for estimating PM₁₀ concentrations in Seoul, as results are significantly affected by the spatial variability of aerosols. The performances of the models for estimating PM₁₀ were also good at midday when aerosols are well mixed within the boundary layer, which suggests a dependence of PM₁₀ estimation on the measurement time.

Seasonal variations in the performances of the empirical models for PM₁₀ estimation were detected. The highest correlation was found using M3 and M5 in winter ($R = 0.81$), when both BLH and the effective radius of the aerosol are considered; the high correlations can be attributed to a lower aerosol mixing height and homogeneity in the optical and microphysical properties of aerosols within the BLH. The poorest performance was found in spring, when the impact of Asian dust events on both inhomogeneous vertical structure of particle number and aerosol composition at the measurement sites is common, and leads to variable effects.

As discussed in this study, the spatial distribution of surface-level PM₁₀ concentrations can be estimated using empirical models. The use of satellite measurements in these various empirical models has the advantage of both simplicity and wide spatial coverage over megacity areas. However, the predictability of PM₁₀ distributions using empirical models should be improved. The performances of empirical models for PM predictions can be improved by using finer spatial resolution satellite data, such as MODIS collection 6 (Levy et al., 2013), Geostationary Ocean Color Imager (GOCI) aerosol products (Lee et al., 2010b), and more detailed information on aerosol composition, size, vertical distribution, and so on. Also, to enhance the accuracy of PM₁₀ estimations in other seasons, further work is required to investigate seasonal effects on the spatial variability of PM₁₀ estimations in Seoul. In addition to the evaluation of multiple empirical models in the megacity area, a chemistry transport model (CTM) should also be performed and validated for PM₁₀ estimations.

Spatio-temporal variations in PM₁₀ concentrations over Seoul

S. Seo et al.

[Title Page](#)
[Abstract](#)
[Introduction](#)
[Conclusions](#)
[References](#)
[Tables](#)
[Figures](#)




[Back](#)
[Close](#)
[Full Screen / Esc](#)
[Printer-friendly Version](#)
[Interactive Discussion](#)


Acknowledgement. This research was supported by the GEMS program of the Ministry of Environment, Korea and the Eco Innovation Program of KEITI (2012000160002). The authors deeply appreciate NIER and the staff for the DRAGON-Asia campaign in establishing and maintaining the AERONET sites. We would also like to thank NIER for the PM₁₀ data used, NASA for the AERONET and MODIS data, and NIES Lidar team for the lidar data. This research was partially supported by the Brain Korea 21 Plus for SS, JK, HL, WJ, and WK.

References

- Baumer, D., Vogel, B., Versick, S., Rinke, R., Mohler, O., and Schnaiter, M.: Relationship of visibility, aerosol optical thickness and aerosol size distribution in an ageing air mass over South-West Germany, *Atmos. Environ.*, 42, 989–998, doi:10.1016/j.atmosenv.2007.10.017, 2008.
- Brauer, M., Amann, M., Burnett, R. T., Cohen, A., Dentener, F., Ezzati, M., Henderson, S. B., Krzyzanowski, M., Martin, R. V., and Van Dingenen, R.: Exposure assessment for estimation of the global burden of disease attributable to outdoor air pollution, *Environ. Sci. Technol.*, 46, 652–660, 2012.
- Brook, R. D., Rajagopalan, S., Pope, C. A., Brook, J. R., Bhatnagar, A., Diez-Roux, A. V., Holguin, F., Hong, Y. L., Luepker, R. V., Mittleman, M. A., Peters, A., Siscovick, D., Smith, S. C., Whitsel, L., Kaufman, J. D., Epidemiol. A. H. A. C., Dis, C. K. C., and Metab, C. N. P. A.: Particulate Matter Air Pollution and Cardiovascular Disease An Update to the Scientific Statement From the American Heart Association, *Circulation*, 121, 2331–2378, 2010.
- Brooks, I. M.: Finding boundary layer top: application of a wavelet covariance transform to lidar backscatter profiles, *J. Atmos. Ocean. Tech.*, 20, 1092–1105, 2003.
- Campbell, J. R., Hlavka, D. L., Welton, E. J., Flynn, C. J., Turner, D. D., Spinhirne, J. D., Scott, V. S., and Hwang, I. H.: Full-time, eye-safe cloud and aerosol lidar observation at atmospheric radiation measurement program sites: instruments and data processing, *J. Atmos. Ocean. Tech.*, 19, 431–442, 2002.
- Chu, D. A., Kaufman, Y. J., Zibordi, G., Chern, J. D., Mao, J., Li, C. C., and Holben, B. N.: Global monitoring of air pollution over land from the Earth Observing System-Terra Moderate Resolution Imaging Spectroradiometer (MODIS), *J. Geophys. Res.-Atmos.*, 108, 4661, doi:10.1029/2002jd003179, 2003.

**Spatio-temporal
variations in PM₁₀
concentrations over
Seoul**

S. Seo et al.

[Title Page](#)[Abstract](#)[Introduction](#)[Conclusions](#)[References](#)[Tables](#)[Figures](#)[Back](#)[Close](#)[Full Screen / Esc](#)[Printer-friendly Version](#)[Interactive Discussion](#)

Dubovik, O. and King, M. D.: A flexible inversion algorithm for retrieval of aerosol optical properties from Sun and sky radiance measurements, *J. Geophys. Res.-Atmos.*, 105, 20673–20696, doi:10.1029/2000jd900282, 2000.

Dubovik, O., Smirnov, A., Holben, B. N., King, M. D., Kaufman, Y. J., Eck, T. F., and Slutsker, I.: Accuracy assessments of aerosol optical properties retrieved from Aerosol Robotic Network (AERONET) Sun and sky radiance measurements, *J. Geophys. Res.-Atmos.*, 105, 9791–9806, doi:10.1029/2000jd900040, 2000.

Emili, E., Popp, C., Petitta, M., Riffler, M., Wunderle, S., and Zebisch, M.: PM₁₀ remote sensing from geostationary SEVIRI and polar-orbiting MODIS sensors over the complex terrain of the European Alpine region, *Remote Sens. Environ.*, 114, 2485–2499, doi:10.1016/j.rse.2010.05.024, 2010.

Engel-Cox, J. A., Holloman, C. H., Coutant, B. W., and Hoff, R. M.: Qualitative and quantitative evaluation of MODIS satellite sensor data for regional and urban scale air quality, *Atmos. Environ.*, 38, 2495–2509, doi:10.1016/j.atmosenv.2004.01.039, 2004.

Engel-Cox, J. A., Hoff, R. M., Rogers, R., Dimmick, F., Rush, A. C., Szykman, J. J., Al-Saadi, J., Chu, D. A., and Zell, E. R.: Integrating lidar and satellite optical depth with ambient monitoring for 3-dimensional particulate characterization, *Atmos. Environ.*, 40, 8056–8067, doi:10.1016/j.atmosenv.2006.02.039, 2006.

Guo, J.-P., Zhang, X.-Y., Che, H.-Z., Gong, S.-L., An, X., Cao, C.-X., Guang, J., Zhang, H., Wang, Y.-Q., and Zhang, X.-C.: Correlation between PM concentrations and aerosol optical depth in eastern China, *Atmos. Environ.*, 43, 5876–5886, 2009.

Gupta, P. and Christopher, S. A.: Seven year particulate matter air quality assessment from surface and satellite measurements, *Atmos. Chem. Phys.*, 8, 3311–3324, doi:10.5194/acp-8-3311-2008, 2008.

Hauck, H., Berner, A., Gomiscek, B., Stopper, S., Puxbaum, H., Kundi, M., and Preining, O.: On the equivalence of gravimetric PM data with TEOM and beta-attenuation measurements, *J. Aerosol Sci.*, 35, 1135–1149, doi:10.1016/j.jaerosci.2004.04.004, 2004.

Holben, B. N., Eck, T. F., Slutsker, I., Tanre, D., Buis, J. P., Setzer, A., Vermote, E., Reagan, J. A., Kaufman, Y. J., Nakajima, T., Lavenu, F., Jankowiak, I., and Smirnov, A.: AERONET – A federated instrument network and data archive for aerosol characterization, *Remote Sens. Environ.*, 66, 1–16, doi:10.1016/S0034-4257(98)00031-5, 1998.

IPCC (Intergovernmental Panel on Climate Change): Climate Change 2013: The Physical Science Basis. Contribution of Working Group I to the Fifth Assessment Report of the Intergov-

Spatio-temporal variations in PM₁₀ concentrations over Seoul

S. Seo et al.

[Title Page](#)
[Abstract](#)
[Introduction](#)
[Conclusions](#)
[References](#)
[Tables](#)
[Figures](#)




[Back](#)
[Close](#)
[Full Screen / Esc](#)
[Printer-friendly Version](#)
[Interactive Discussion](#)


- Levy, R. C., Mattoo, S., Munchak, L. A., Remer, L. A., Sayer, A. M., Patadia, F., and Hsu, N. C.: The Collection 6 MODIS aerosol products over land and ocean, *Atmos. Meas. Tech.*, 6, 2989–3034, doi:10.5194/amt-6-2989-2013, 2013.
- Liu, Y., Park, R. J., Jacob, D. J., Li, Q. B., Kilaru, V., and Sarnat, J. A.: Mapping annual mean ground-level PM_{2.5} concentrations using Multiangle Imaging Spectroradiometer aerosol optical thickness over the contiguous United States, *J. Geophys. Res.-Atmos.*, 109, D22206, doi:10.1029/2004jd005025, 2004.
- Liu, Y., Sarnat, J. A., Kilaru, V., Jacob, D. J., and Koutrakis, P.: Estimating ground-level PM_{2.5} in the eastern United States using satellite remote sensing, *Environ. Sci. Technol.*, 39, 3269–3278, 2005.
- Liu, Y., Franklin, M., Kahn, R., and Koutrakis, P.: Using aerosol optical thickness to predict ground-level PM_{2.5} concentrations in the St. Louis area: A comparison between MISR and MODIS, *Remote Sens. Environ.*, 107, 33–44, doi:10.1016/j.rse.2006.05.022, 2007.
- Murayama, T., Sugimoto, N., Uno, I., Kinoshita, K., Aoki, K., Hagiwara, N., Liu, Z. Y., Matsui, I., Sakai, T., Shibata, T., Arai, K., Sohn, B. J., Won, J. G., Yoon, S. C., Li, T., Zhou, J., Hu, H. L., Abo, M., Iokibe, K., Koga, R., and Iwasaka, Y.: Ground-based network observation of Asian dust events of April 1998 in east Asia, *J. Geophys. Res.-Atmos.*, 106, 18345–18359, 2001.
- Ogunjobi, K. O., Kim, Y. J., and He, Z.: Influence of the total atmospheric optical depth and cloud cover on solar irradiance components, *Atmos. Res.*, 70, 209–227, doi:10.1016/j.atmosres.2004.01.003, 2004.
- Pan, X. L., Yan, P., Tang, J., Ma, J. Z., Wang, Z. F., Gbaguidi, A., and Sun, Y. L.: Observational study of influence of aerosol hygroscopic growth on scattering coefficient over rural area near Beijing mega-city, *Atmos. Chem. Phys.*, 9, 7519–7530, doi:10.5194/acp-9-7519-2009, 2009.
- Pelletier, B., Santer, R., and Vidot, J.: Retrieving of particulate matter from optical measurements: a semiparametric approach, *J. Geophys. Res.-Atmos.*, 112, D06208, doi:10.1029/2005JD006737, 2007.
- Pope, C. A., Burnett, R. T., Thun, M. J., Calle, E. E., Krewski, D., Ito, K., and Thurston, G. D.: Lung cancer, cardiopulmonary mortality, and long-term exposure to fine particulate air pollution, *JAMA-J. Am. Med. Assoc.*, 287, 1132–1141, 2002.
- Remer, L. A., Kaufman, Y. J., Tanre, D., Mattoo, S., Chu, D. A., Martins, J. V., Li, R. R., Ichoku, C., Levy, R. C., Kleidman, R. G., Eck, T. F., Vermote, E., and Holben, B. N.: The MODIS aerosol algorithm, products, and validation, *J. Atmos. Sci.*, 62, 947–973, 2005.

**Spatio-temporal
variations in PM₁₀
concentrations over
Seoul**

S. Seo et al.

Title Page

Abstract

Introduction

Conclusions

References

Tables

Figures

⏪

⏩

◀

▶

Back

Close

Full Screen / Esc

Printer-friendly Version

Interactive Discussion



Schaap, M., Apituley, A., Timmermans, R. M. A., Koelemeijer, R. B. A., and de Leeuw, G.: Exploring the relation between aerosol optical depth and PM_{2.5} at Cabauw, the Netherlands, *Atmos. Chem. Phys.*, 9, 909–925, doi:10.5194/acp-9-909-2009, 2009.

van Donkelaar, A., Martin, R. V., Brauer, M., Kahn, R., Levy, R., Verduzco, C., and Villeneuve, P. J.: Global estimates of ambient fine particulate matter concentrations from satellite-based aerosol optical depth: development and application, *Environ. Health Persp.*, 118, 847–855, doi:10.1289/ehp.0901623, 2010.

Wang, J. and Christopher, S. A.: Intercomparison between satellite-derived aerosol optical thickness and PM_{2.5} mass: Implications for air quality studies, *Geophys. Res. Lett.*, 30, 2095, doi:10.1029/2003gl018174, 2003.

Wang, Z. F., Chen, L. F., Tao, J. H., Zhang, Y., and Su, L.: Satellite-based estimation of regional particulate matter (PM) in Beijing using vertical-and-RH correcting method, *Remote Sens. Environ.*, 114, 50–63, doi:10.1016/j.rse.2009.08.009, 2010.

WHO (World Health Organization): WHO Air quality guidelines for particulate matter, ozone, nitrogen dioxide and sulfur dioxide - global update 2005, WHO Press, World Health Organization, Geneva, Switzerland, 2005.

Spatio-temporal variations in PM₁₀ concentrations over Seoul

S. Seo et al.

Title Page

Abstract

Introduction

Conclusions

References

Tables

Figures

◀

▶

◀

▶

Back

Close

Full Screen / Esc

Printer-friendly Version

Interactive Discussion



Table 1. Previous studies associated with the estimation of PM concentrations using AOD.

Method	Study area	Data		<i>R</i>	Reference
		AOD	PM _x		
M1 ^a	Northern Italy	Daily Sunphotometer	Daily PM ₁₀	0.82	Chu et al. (2003)
M1	Alabama	MODIS (10 km)	PM _{2.5}	0.70	Wang and Christopher. (2003)
M1	Southeastern US	MODIS (10 km)	PM _{2.5}	0.40	Engel-Cox et al. (2004)
M1	US	MODIS	Daily PM _{2.5}	0.43	
			PM _{2.5}	0.52	Gupta and Christopher. (2008)
			Daily PM _{2.5}	0.62	
M1	Cabauw	Sunphotometer	PM _{2.5}	0.75	Schaap et al. (2009)
		MODIS (10 km)		0.72	
M2 ^b	Europe	MODIS (10 km)	PM _{2.5}	0.60	Koelemeijer et al. (2006)
			PM ₁₀	0.50	
M2	Alpine region	SEVIRI	Daily PM ₁₀	0.70	Emili et al. (2010)
		MODIS		0.60	
M2	Beijing	MODIS (1 km)	PM _{2.5}	0.68	Wang et al. (2010)
			PM ₁₀	0.68	
M3 ^c	Eastern US	MISR	Daily PM _{2.5}	0.69	Liu et al. (2005)
M3	St. Louis	MISR	Daily PM _{2.5}	0.79	Liu et al. (2007)
		MODIS		0.71	
M3	Lille	Sunphotometer	PM ₁₀	0.87	Pelletier et al. (2007)
M4 ^d	US	MISR	Yearly PM _{2.5}	0.78	Liu et al. (2004)

^a M1 uses the empirical linear relationship between AOD and PM_x ($PM_x = aAOD + b$).

^b M2 uses the empirical linear relationship between corrected AOD (vertical distribution, RH) and PM_x.

^c M3 uses the poly-parameter model.

^d M4 uses the 3-D atmospheric chemistry model.

Spatio-temporal variations in PM₁₀ concentrations over Seoul

S. Seo et al.

Table 2. Statistical summary of AOD and cloud screened AOD (AOD_{cl}) observed by AERONET and MODIS during the DRAGON-Asia campaign period.

	AERONET		MODIS	
	AOD	AOD _{cl}	AOD	AOD _{cl}
Mean ± std	0.51 ± 0.34	0.42 ± 0.26	0.74 ± 0.38	0.73 ± 0.37
Min	0.09	0.09	0.03	0.03
Median	0.43	0.35	0.72	0.68
Max	2.99	1.42	1.94	1.94
<i>N</i>	3406	2112	292	252

Title Page

Abstract

Introduction

Conclusions

References

Tables

Figures



Back

Close

Full Screen / Esc

Printer-friendly Version

Interactive Discussion



Spatio-temporal variations in PM₁₀ concentrations over Seoul

S. Seo et al.

[Title Page](#)[Abstract](#)[Introduction](#)[Conclusions](#)[References](#)[Tables](#)[Figures](#)[⏪](#)[⏩](#)[◀](#)[▶](#)[Back](#)[Close](#)[Full Screen / Esc](#)[Printer-friendly Version](#)[Interactive Discussion](#)

Table 3. The empirical linear models used for PM₁₀ estimations in this study.

Model	Model description	Application
M1	$PM_{10} = aAOD + b$	AERONET, MODIS
M2	$PM_{10} = a \frac{AOD}{BLH} + b$	AERONET, MODIS
M3	$PM_{10} = a \frac{AOD \times R_{eff}}{BLH} + b$	AERONET
M4	$PM_{10} = a \frac{AOD}{BLH \times f(RH)} + b$	AERONET, MODIS
M5	$PM_{10} = a \frac{AOD \times R_{eff}}{BLH \times f(RH)} + b$	AERONET
M6	Sect. 3.2 Eq. (5) (multiple linear regression model)	AERONET

Spatio-temporal variations in PM₁₀ concentrations over Seoul

S. Seo et al.

Title Page

Abstract

Introduction

Conclusions

References

Tables

Figures

◀

▶

◀

▶

Back

Close

Full Screen / Esc

Printer-friendly Version

Interactive Discussion



Table 4. Estimated regression coefficients for the multiple linear regression model (M6) (described in Sect. 3.2, Eq. 5) using AERONET data ($N = 1058$).

Model parameter	Estimate	Standard error	p value
Intercept	4.363	0.080	< 0.0001
ln(AOD)	0.527	0.022	< 0.0001
ln(BLH)	-0.280	0.028	< 0.0001
ln(AE)	0.066	0.033	0.047
Location type			
Near source	0.233	0.032	< 0.0001
Urban	0.013	0.032	0.684
Suburban	0.000	–	–
Wind speed	0.015	0.008	0.052
Wind direction			
From the north	0.205	0.054	< 0.0001
From the south	0.164	0.045	< 0.0001
From the west	0.307	0.036	< 0.0001
From the east	0.000	–	–
RH	-0.610	0.116	< 0.0001
Temperature	-0.010	0.002	< 0.0001

Spatio-temporal variations in PM₁₀ concentrations over Seoul

S. Seo et al.

[Title Page](#)
[Abstract](#)
[Introduction](#)
[Conclusions](#)
[References](#)
[Tables](#)
[Figures](#)
[Back](#)
[Close](#)
[Full Screen / Esc](#)
[Printer-friendly Version](#)
[Interactive Discussion](#)


Table 6. Spatial variations of the correlation coefficient (R), root mean square error (RMSE), mean normalized bias (MNB), and mean fractionalized bias (MFB) between measured PM₁₀ concentrations and those estimated from the different empirical linear models for the three different site categories, using the data collected by AERONET and MODIS, during the DRAGON-Asia campaign period in Seoul.

Performance of empirical models used to estimate hourly PM ₁₀ using AERONET datasets with respect to model and measurement site types							
		Model M1 _{cl}	M2	M3	M4	M5	M6
NS	R	0.49	0.57 (0.49)	0.59	0.57 (0.49)	0.61	0.61
	N	807	807 (237)	237	807 (237)	237	190
	RMSE ($\mu\text{g m}^{-3}$)	26.29	24.79 (26.90)	24.79	24.67 (26.79)	24.28	22.85
	MNBE (%)	21.21	20.54 (27.32)	24.57	20.38 (26.95)	23.48	7.12
	MFB (%)	9.03	8.56 (15.21)	13.05	8.65 (15.05)	12.35	-0.37
TU	R	0.51	0.60 (0.43)	0.61	0.61 (0.45)	0.64	0.72
	N	891	891 (367)	367	891 (367)	367	190
	RMSE ($\mu\text{g m}^{-3}$)	22.61	21.11 (21.77)	19.06	20.94 (21.50)	18.43	17.69
	MNBE (%)	24.27	24.25 (23.91)	20.26	23.47 (22.67)	18.46	4.16
	MFB (%)	10.09	9.84 (6.14)	5.39	9.88 (5.78)	4.86	-1.85
RA	R	0.63	0.73 (0.63)	0.69	0.73 (0.64)	0.70	0.76
	N	414	414 (109)	109	414 (109)	109	92
	RMSE ($\mu\text{g m}^{-3}$)	19.67	17.35 (18.02)	16.92	17.26 (17.81)	16.53	17.09
	MNBE (%)	17.31	16.08 (25.85)	22.60	15.32 (25.19)	21.52	5.99
	MFB (%)	8.15	7.26 (13.61)	12.08	6.94 (13.41)	11.62	0.47

Spatio-temporal variations in PM₁₀ concentrations over Seoul

S. Seo et al.

Table 6. Continued.

		Performance of empirical models used to estimate hourly PM ₁₀ using AERONET datasets with respect to model and measurement site types					
		M1 _{cl}	M2	Model		M5	M6
				M3	M4		
		Performance of empirical models to estimate hourly PM ₁₀ using MODIS datasets with respect to model and measurement site types					
		M1 _{cl}	M2	Model		M5	M6
				M3	M4		
NS	<i>R</i>	0.37	0.68	–	0.68	–	–
	<i>N</i>	105	105	–	105	–	–
	RMSE (μg m ⁻³)	32.09	27.34	–	27.32	–	–
	MNBE (%)	24.93	16.10	–	15.98	–	–
	MFB (%)	10.80	6.99	–	7.04	–	–
TU	<i>R</i>	0.42	0.72	–	0.71	–	–
	<i>N</i>	95	95	–	95	–	–
	RMSE (μg m ⁻³)	26.41	20.08	–	20.45	–	–
	MNBE (%)	21.23	15.23	–	15.58	–	–
	MFB (%)	9.42	6.55	–	6.78	–	–
RA	<i>R</i>	0.50	0.76	–	0.74	–	–
	<i>N</i>	52	52	–	52	–	–
	RMSE (μg m ⁻³)	23.66	17.93	–	18.33	–	–
	MNBE (%)	17.36	11.40	–	11.57	–	–
	MFB (%)	7.96	4.93	–	5.04	–	–

Title Page

Abstract Introduction

Conclusions References

Tables Figures

⏪ ⏩

◀ ▶

Back Close

Full Screen / Esc

Printer-friendly Version

Interactive Discussion



Spatio-temporal variations in PM₁₀ concentrations over Seoul

S. Seo et al.

[Title Page](#)
[Abstract](#)
[Introduction](#)
[Conclusions](#)
[References](#)
[Tables](#)
[Figures](#)
[Back](#)
[Close](#)
[Full Screen / Esc](#)
[Printer-friendly Version](#)
[Interactive Discussion](#)


Table 7. Seasonal variations of the correlation coefficient (R) and root mean square error (RMSE) between measured PM₁₀ concentrations and those estimated by the different empirical linear models using AERONET datasets, collected at Yonsei University for 17 months.

		Performance of empirical models to estimate hourly PM ₁₀ using AERONET datasets with respect to model and season				
		Model				
		M1 _{cl}	M2	M3	M4	M5
Spring	R	0.39	0.47 (0.45)	0.48	0.48 (0.46)	0.54
	N	465	465 (142)	142	465 (142)	142
	RMSE ($\mu\text{g m}^{-3}$)	41.17	39.60 (29.39)	28.77	39.37 (29.16)	27.76
Summer	R	0.70	0.67 (0.64)	0.64	0.71 (0.67)	0.66
	N	85	85 (21)	21	85 (21)	21
	RMSE ($\mu\text{g m}^{-3}$)	13.85	14.39 (13.75)	13.60	13.81 (13.13)	10.39
Autumn	R	0.60	0.64 (0.52)	0.54	0.66 (0.57)	0.58
	N	212	212 (99)	99	212 (99)	99
	RMSE ($\mu\text{g m}^{-3}$)	13.41	12.89 (14.86)	14.71	12.66 (14.32)	14.17
Winter	R	0.63	0.70 (0.70)	0.81	0.70 (0.70)	0.81
	N	284	284 (116)	116	284 (116)	116
	RMSE ($\mu\text{g m}^{-3}$)	19.81	18.17 (21.16)	17.44	18.10 (21.01)	17.29

Spatio-temporal variations in PM₁₀ concentrations over Seoul

S. Seo et al.

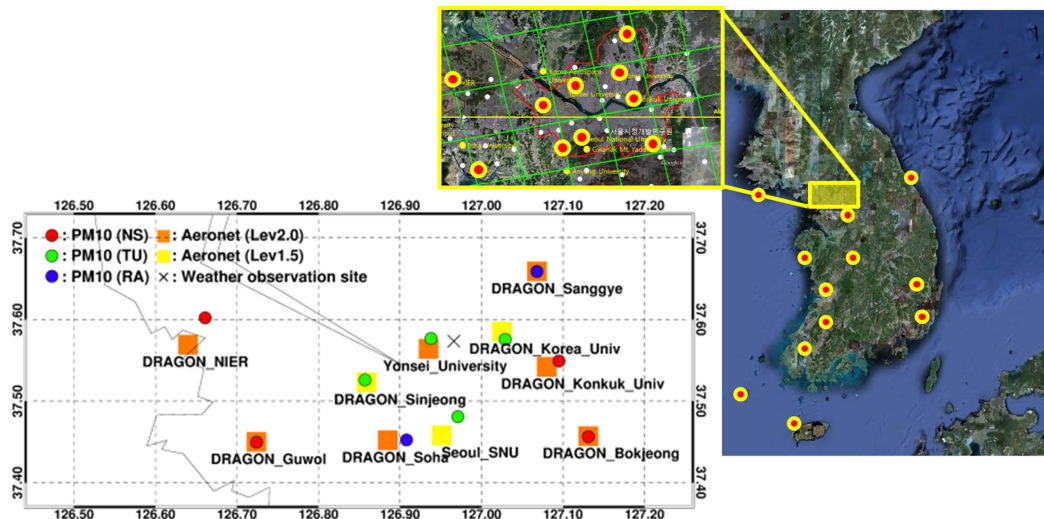


Figure 1. The spatial distribution of AERONET stations, PM₁₀ monitoring sites, and weather observation sites across the Seoul metropolitan area. Orange and yellow boxes indicate the locations of AERONET level 2.0 and 1.5 sites, respectively. The colored circles denote the locations of PM₁₀ monitoring sites. Red, green, and blue sites represent near source (NS), typical urban (TU), and residential area (RA) site types, respectively.

[Title Page](#)
[Abstract](#)
[Introduction](#)
[Conclusions](#)
[References](#)
[Tables](#)
[Figures](#)
[Back](#)
[Close](#)
[Full Screen / Esc](#)
[Printer-friendly Version](#)
[Interactive Discussion](#)

Spatio-temporal variations in PM₁₀ concentrations over Seoul

S. Seo et al.

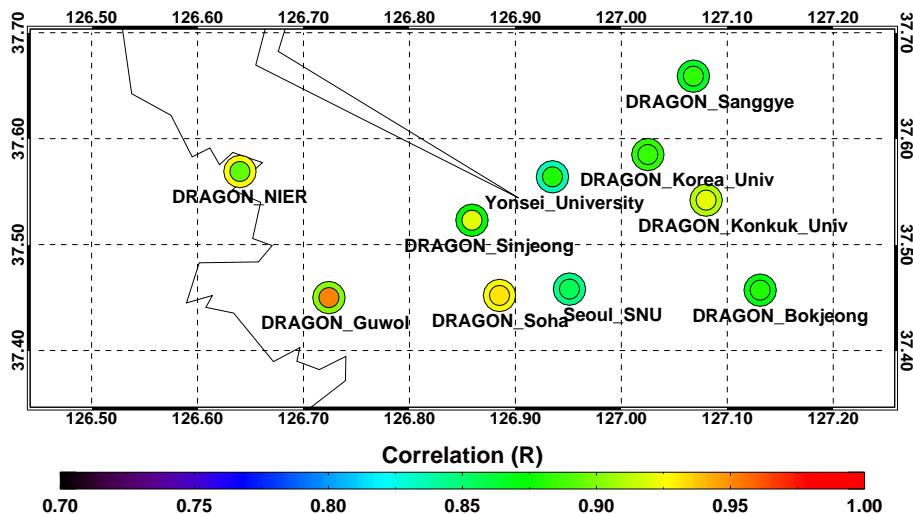


Figure 2. The distribution of correlation coefficients between AERONET AOD and MODIS AOD at 0.55 μm with respect to different spatial resolutions. The inner (outer) circle indicates the correlation between AERONET AOD and MODIS AOD with a resolution of 10 km (30 km).

Spatio-temporal variations in PM₁₀ concentrations over Seoul

S. Seo et al.

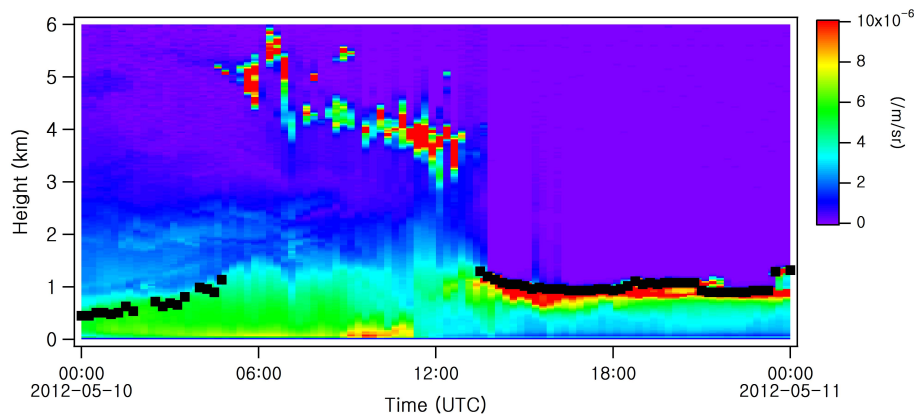


Figure 3. Time plot of attenuated backscatter coefficients observed from the two-wavelength Mie lidar at Seoul National University, and boundary layer height (marked by black squares) retrieved by the automated wavelet covariance transform (WCT) method of Brooks (2003).

[Title Page](#)[Abstract](#)[Introduction](#)[Conclusions](#)[References](#)[Tables](#)[Figures](#)[◀](#)[▶](#)[◀](#)[▶](#)[Back](#)[Close](#)[Full Screen / Esc](#)[Printer-friendly Version](#)[Interactive Discussion](#)

Spatio-temporal variations in PM₁₀ concentrations over Seoul

S. Seo et al.

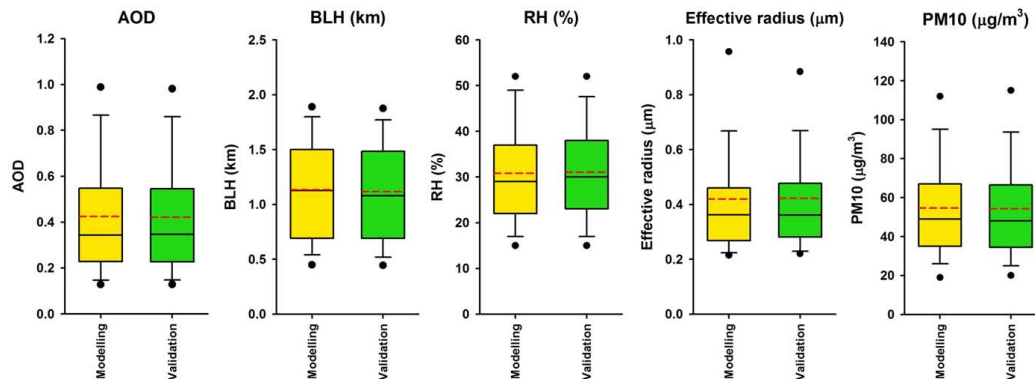


Figure 4. The distribution (5 %, 10 %, 25 %, median, 75 %, 90 %, and 95 %) of AOD, boundary layer height (BLH), relative humidity (RH), effective radius, and PM₁₀ concentrations in the modelling and validation groups derived from AERONET datasets collected during the DRAGON-Asia campaign in Seoul. The red dashed line in the plot denotes the mean value.

[Title Page](#)[Abstract](#)[Introduction](#)[Conclusions](#)[References](#)[Tables](#)[Figures](#)[Back](#)[Close](#)[Full Screen / Esc](#)[Printer-friendly Version](#)[Interactive Discussion](#)

Spatio-temporal variations in PM₁₀ concentrations over Seoul

S. Seo et al.

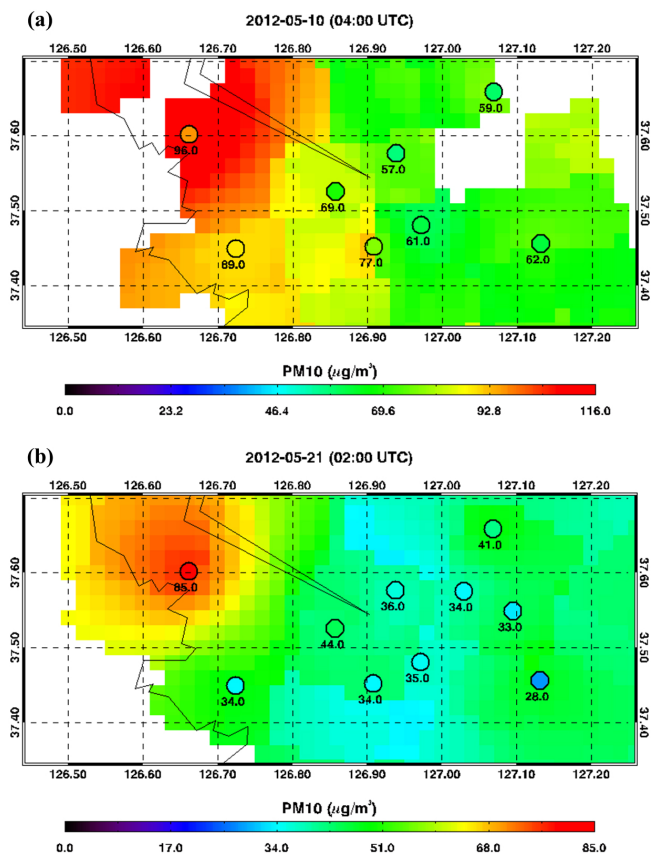


Figure 5. Distribution of hourly surface PM₁₀ concentrations estimated by model M2 using the MODIS datasets for **(a)** 4 UTC, 10 May 2012 and **(b)** 2 UTC, 21 May 2012. Circles indicate the observed PM₁₀ concentrations at PM monitoring sites.